Magnetic Properties of Un-doped and Fe-doped ZnS Thin Films

M Saeed Akhtar[1], Saira Riaz[2], S Sajjad Hussain[3] and Shahzad Naseem[4]

[1], [2], [3], [4] *Centre of Excellence in Solid State Physics, University of the Punjab, Lahore 54590, Pakistan*
[1] *Department of Chemistry, UMIST, UK*
1) saeed_khakhi@yahoo.com

ABSTRACT

The un-doped and Fe-doped ZnS nanocrystalline thin films were deposited on glass substrates by chemical bath deposition (CBD). Iron chloride, zinc chloride and thioacetamide were used as precursors and de-ionized water was used as solvent. The synthesis and deposition of thin films was carried out without using any surfactant/capping agent. The powder X-ray diffraction patterns reveal the formation of cubic zinc blende phase of ZnS in all cases. The incorporation of iron in ZnS lattice was confirmed by the change in lattice parameters accordingly with doping concentration and absence of traces of secondary phases or Fe clusters. The M-H curves indicate that doped ZnS thin films exhibit room temperature ferromagnetism. The magnetization properties as a function of field angle and doping concentration were studied in detail. The density functional calculations were performed using Full Potential Linearized Augmented Plane Wave (FPLAPW) as is employed in elk-code. The strong p-d hybridization observed between sulphur and iron result in ferromagnetic stable state and half metallicity in these materials. The half metallic iron doped ZnS thin films can have applications in future spintronic devices.

1. INTRODUCTION

The research interest is focused during the last decade on the experimental and theoretical study of DMSs offering T_c above room temperature. The T_c of II-VI semiconductors (ZnS and CdS) based DMS is found to be very close to room temperature and can be adjusted by the different synthesis parameters especially the dopant concentration. The Mn doped InAs was reported as DMS with T_c above room temperature (Holub 2004). The ZnS being an important II–VI compound semiconductor with direct wide band gap may be expected to be ferromagnetic at room temperature. The transition metal doped ZnS are found to be half metallic when doped with Cr, Fe, and Ni while maintain its semiconducting nature when doped with Mn and Co (Stern 2004 and McNorton 2008). Tablero (2006) found that ZnS doped with Cr has a partially filled intermediate band for both FM and AFM spin alignments.

---

[1] Graduate Student
[2], [3], [4] Professor

Most recently, there are several reports on theoretical and experimental evidences of room temperature ferromagnetism and half metallicity in transition metal doped ZnS nanoparticles and nanowires. The room temperature ferromagnetism in ZnFeS nanoparticles obtained via chemical co-precipitation was reported first time by Sambasivam (2008). Up to now various chemical methods have been adopted to synthesize iron doped ZnS nanoparticles and nanocrystals such as; microemulsion method (Li 2011), chemical co-precipitation (Nie 2011, Chauhan 2013) and hydrothermal method (Cao 2013, Wei 2013). On the basis of theoretical studies, Xie (2010) reported ferromagnetism and half metallicity in transition metals doped ZnS by DFT studies and found that the magnetic moments due to 3d orbitals of transition metal ions are delocalized on the ions of host semiconductors. The long range interactions resulted from induced magnetic moments of transition metal ions are responsible for ferromagnetism and half metallicity in host material. Chen (2011) proposed that strong p-d hybridization between sulfur and transition metal ions results in ferromagnetic coupling. They studied both substitutional and interstitial doping theoretically in ZnS cluster via DFT. There are few reports on investigation of room temperature ferromagnetism in iron doped ZnS thin films by any of the technique. Zhu (2010) observed the T_c of 270K in iron doped ZnS thin films deposited on GaAs substrates by metal organic chemical vapor deposition (MOCVD). The probable effect of size distribution on structural and magnetic properties of ZnFeS nanoparticles was investigated.

These reports have aroused interest of the present authors to use chemical synthesis technique i.e. chemical bath deposition but without a surface capping or complexing agent. To the best of our knowledge, the magnetic studies on iron doped ZnS thin films deposited by CBD method yet not reported.

Here in, we report the capping agent free deposition of nanocrystalline iron doped ZnS thin films by CBD method. The structural, morphological and magnetic properties of deposited thin films have been studied. We also compare our experimental findings with DFT calculation on iron doped ZnS cubic zinc blende clusters using elk-code in close proximity regarding doping concentration used in experiments.

2. EXPERIMENTAL DETAILS

Un-doped and iron doped ZnS thin films were deposited on glass substrates by CBD method at acidic value of pH (4.0). Appropriate quantities of zinc chloride, iron chloride and thioacetamide were weighed according to the stoichiometry and were dissolved in deionized water to make 0.2, 0.2 and 0.4M solutions respectively. The aqueous solution of thioacetamide was mixed drop wise to that of zinc chloride under vigorous stirring with magnetic stirrer at room temperature. Nitric acid (0.5M) was used to control the pH of solution. After complete dissolution of thioacetamide in zinc chloride, transparent solution was obtained. At this stage, suitable volumes of iron chloride solution depending on the desired doping concentration were added drop wise to the solution containing zinc chloride and tthioacetamide. It is worth mentioning that the whole synthesis was performed without use of any surfactant or capping agent. After complete dissolution of iron chloride, the final solution was transferred to chemical bath and maintained at 80°C under magnetic stirring. After half an hour the color of solution

turned light brown showing the incorporation of iron in ZnS lattice. The pre-cleaned glass substrates were immersed vertical in the chemical bath at this stage and removed after three hours. After removal from the baths, the substrates were washed with de-ionized water and any loosely bound precipitates were removed by ultrasonic agitation. After deposition, all the samples were dried in ambient atmosphere and then annealed in nitrogen for one hour at 400°C to remove any organic byproducts formed during the reaction process.

3. COMPUTATIONAL DETAILS

Full Potential Linearized Augmented Plane Wave (FPLAPW) approach was used to solve Kohn-Sham equation within Density Functional Theory (Kohn 1965, Hohenberg 1964) formulation as is employed in elk-code in order to investigate the electronic and magnetic properties of $Zn_{1-x}Fe_xS$ alloys, Generalized Gradient Approximation plus PBE (Perdew 1996) along with Hubbard functional U (GGA-PBE+U) is used for optimization of the exchange correlation energy. Inside the non-overlapping spheres surrounding the atomic sites (muffin-tin spheres) the wave functions are expanded into spherical harmonics with angular momentum quantum number lmax = 10 and in the interstitial region, wave functions are expanded into plane wave basis. A plane wave cutoff of rgkmax = 7 is used for the expansion of wave functions inside the interstitial regions. The cutoff for reciprocal vector of Fourier expansion i.e. gmaxvr is set to 14 and actual value for smearing swidth = 0.001. Maximum 'G' for potential and density is fixed at 12. Maximum angular momentum used for APW functions was 8 and effective Wigner radius is fixed to 0.65Å. The muffin-tin radii RMT's are fixed at value of 1.058Å so that there is no charge leakage from the core and total energy convergence is ensured. Spin orbit coupling is considered to observe spin polarization. Complex Hermitian eigen solver will be used since the crystal has no inversion symmetry. A dense uniformly distributed mesh of 4×4×4 k-points is used in the irreducible part of Brillouin Zone ensuring that the Brillouin Zone is densely populated. The core electrons are treated fully relativistically by solving the Dirac equation, whereas the valence electrons are treated non-relativistically. Furthermore, we have included the structure optimization to relax the internal atomic positions upon deformations.

4. RESULTS AND DISCUSSION

4.1 Structural studies

The XRD patterns (fig. 1) show the poly and nanocrystalline nature of Fe doped ZnS thin films. The observed diffraction peaks correspond to (111), (220) and (311) lattice planes and are well matched with the standard pattern of cubic zinc blende ZnS (ICCD # 01-005-0566). It is well known that ionic radius of Fe^{2+} (0.77 Å) is close to that of Zn^{2+} (0.74 Å), and therefore it is judicious to speculate that it is easy for Fe^{2+} to penetrate in ZnS lattice or to substitute the Zn^{2+}. The Effect of Fe incorporation in ZnS is evident from shift of diffraction peak corresponding to (111) plane from standard 2θ of 28.86° to the smaller 2θ values, since the ionic radii of Fe is slightly bigger than that of Zn.

The shift of diffraction peak (111) is given in table 1. The change in lattice constant of ZnS resulted from iron incorporation was also observed. The Substitution of Fe

(dopant) into the ZnS lattice is indicated as no diffraction peaks corresponding to Fe, FeS and any other impurity were detected. The XRD results reveal that the crystallinity of ZnS thin films decreases as the dopant's concentration increases. This observation is consistent to the investigations of Li (2011). The deposited ZnS thin films have stable cubic phase, even at high doping level no phase transformation is observed unlike the previous report about copper doping in ZnS by Datta (2008).
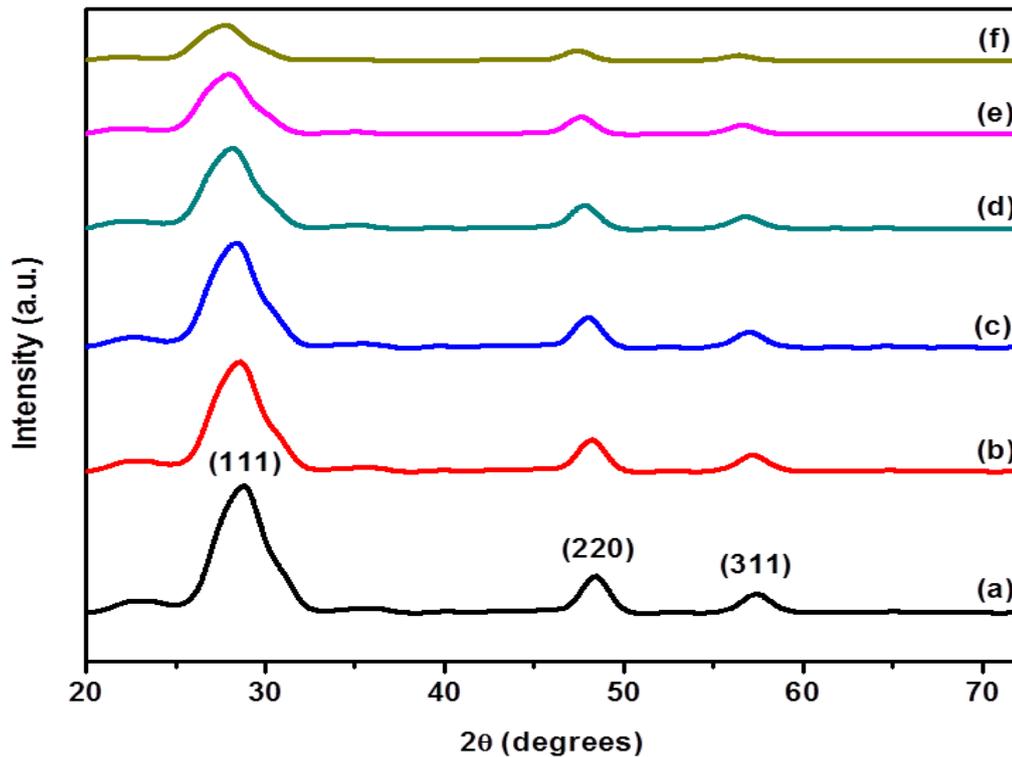
Fig. 1 XRD patterns of un-doped and Fe doped ZnS thin films (a) un-doped, (b) 3% Fe, (c) 6% Fe, (d) 9% Fe, (e) 12% Fe and (f) 15% Fe

The broad diffraction peaks for all the samples indicate that the deposited thin films are composed of nanoparticles. The average crystallite size was estimated by using Scherrer's formula as:

$$D = k\lambda/\beta\cos\theta \qquad\qquad (1)$$

where D is the average crystallite size, k is the geometric factor, λ is the X-ray wavelength of Cu Kα radiations (1.5405Å), β is the full width at half maximum of diffraction peaks, and θ is the Bragg diffraction angle. Furthermore, the absence of iron or impurity peaks indicates that the deposited thin films have single phase and the stoichiometric amounts of iron used in synthesis are completely soluble within the ZnS lattice.

4.2 Morphological studies

SEM representative images (fig. 2) of the ZnFeS thin film show the morphology of un-doped and Fe-doped ZnS thin films. The almost spherical agglomerates assembled of nanoparticles/grains are distributed throughout the surface of the substrate as shown in Fig. 2 (a) for un-doped ZnS thin film. It was observed that agglomeration of nanocrystallites leads to the formation of spherical clusters having an average diameter of 150 nm onto the substrate surface. The uniform layered growth of ZnS is associated with the increase in size of particles instead of more pronounced nucleation (Bayer 2002). The morphology features shown in fig. 2 reveals that at the same conditions, iron doping apparently reduces the crystallinity and grain size was observed to be decreased as the concentration of iron increases in accordance to the XRD measurements (fig. 2 (b-f)). The growth in all the cases is quite similar resulting in agglomerated grains/clusters except enough variation in size but slight variation in shape. Here, it is worth mentioning that, the morphology of thin films was controlled by the optimized growth conditions instead of using any additional surfactant or capping agent. The average particle size obtained from SEM images for un-doped and iron doped ZnS thin films is in the range of 65 to 150 nm. For further and exact calculation of crystallites TEM measurements are needed since the resolution limits of scanning electron microscopy.
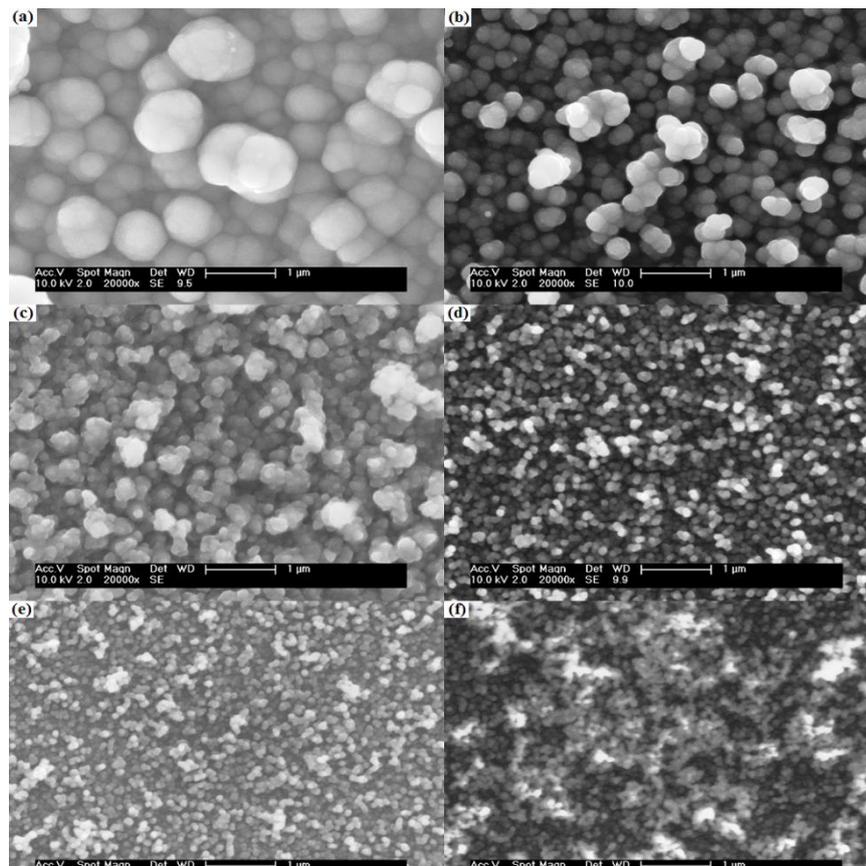
Fig. 2 SEM images of un-doped and Fe doped ZnS thin films (a) un-doped, (b) 3% Fe, (c) 6% Fe, (d) 9% Fe, (e) 12% Fe and (f) 15% Fe

4.3 Magnetic studies

Figure 3 shows the magnetic hysteresis loop of the ZnFeS thin film for the doping concentration of 9% obtained from vibrating sample magnetometer. The ferromagnetism at room temperature can be observed, indicating the Curie temperature for prepared samples above room temperature. In the present study, Zener's p-d hybridization (Akai 2000) is used to explain the magnetic coupling in iron doped ZnS thin films. Although, there is a distinct hysteresis loop observed but the magnetization could not attain the saturation and at higher values of applied magnetic field the M-H curve looks linear with a slope. This behavior of M-H curve at higher magnetization indicates the presence of paramagnetic contribution to the magnetization. The retentively is found to be 9.470×10^{-5} emu and coericivity is 560 Oe.
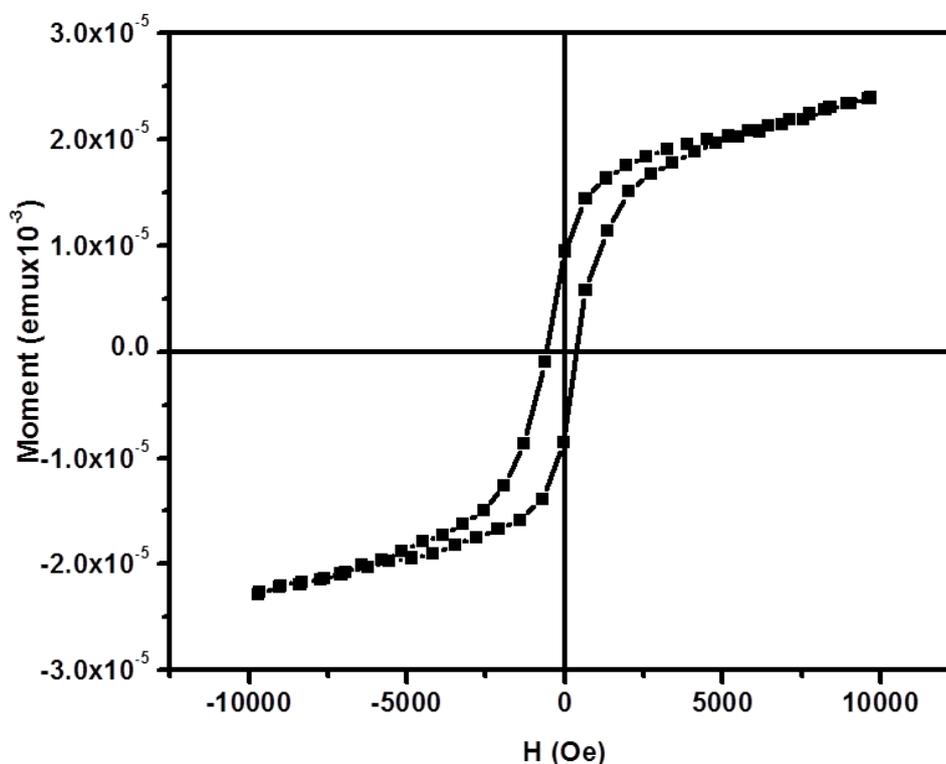
Fig. 3 The M-H loop of ZnFeS thin film for 9% iron

4.4 Geometry optimization

The structural parameters and interatomic positions for ZnS structures with different iron doping are fully optimized. The structure of iron doped ZnS in cubic zinc blende phase was optimized first for 2×2×2 supercells having 64 atoms. The iron doping was carried out by substituting zinc atoms with iron at different positions to achieve desired doping concentration. Fig. 4 shows the un-doped and iron doped ZnS supercells. The lattice parameters obtained are slightly higher than that of pure ZnS in accordance to the lattice parameters obtained experimentally. The difference in ground state energy of

ferromagnetic and antiferromagnetic state is found to be positive, which means that the ferromagnetic state is stable state in iron doped ZnS.
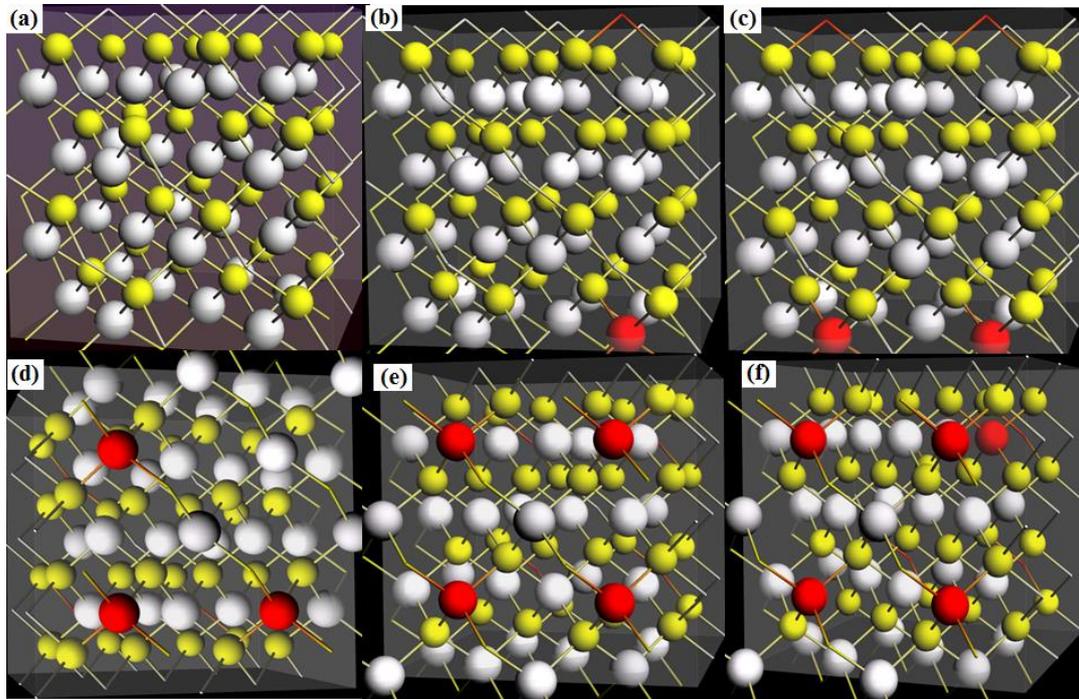
Fig. 4 Supercells (2×2×2) of un-doped and iron doped ZnS (a) un-doped, (b) 3.125% Fe, (c) 6.25% Fe, (d) 9.375% Fe, (e) 12.50% Fe and (f) 15.625% Fe

4.5 Density of states

In the present study, the ferromagnetism in iron doped ZnS can be explained by a strong p-d hybridization between 3p orbital of sulfur and 3d orbital of iron. This kind of coupling is previously reported in dilute magnetic semiconductors according to Zener's p-d hybridization (Akai 2000). This mechanism suggests that the partially occupied states have been introduced by the dopant into the band gap of host material. The total densities of states of un-doped ZnS and with different doping concentrations of iron are shown in fig. 5. The upper part of valence band is dominated by p-states from S atoms while the lower part is attributed to the Zn s-states with a small contribution of S p-states. On the other hand, lower part of conduction band is dominated by s-states of Zn and Fe with some contribution from Zn p-states. The density of states within the band gap in case of iron doped ZnS mainly come from the p-d hybridization of S 3p and Fe 3d orbital. The semiconducting and non-polarized nature of un-doped ZnS is shown in fig. 5 (a), since the spin up and spin down states are identical in un-doped ZnS. The direct band gap of 2.74 eV between HOMO and LUMO is observed which is slightly less than its experimental counterpart due to underestimation when calculated through DFT. When the ZnS is doped with iron (3.125 %) (fig. 5b), presence of density of states for spin up channel in the HOMO-LUMO gap results in reduction of bad gap and is evidence for half metallic behavior while spin down channel remains semiconducting. Due to aforementioned strong p-d hybridization, the majority states shifted towards Fermi level. The 3p state of sulfur contributes to the unoccupied states along with 3d

states of iron. The number of spin up states within the Fermi level increases as the concentration of iron increases beyond the 9.375%, which lowers the total energy of the system (Akai 1998).
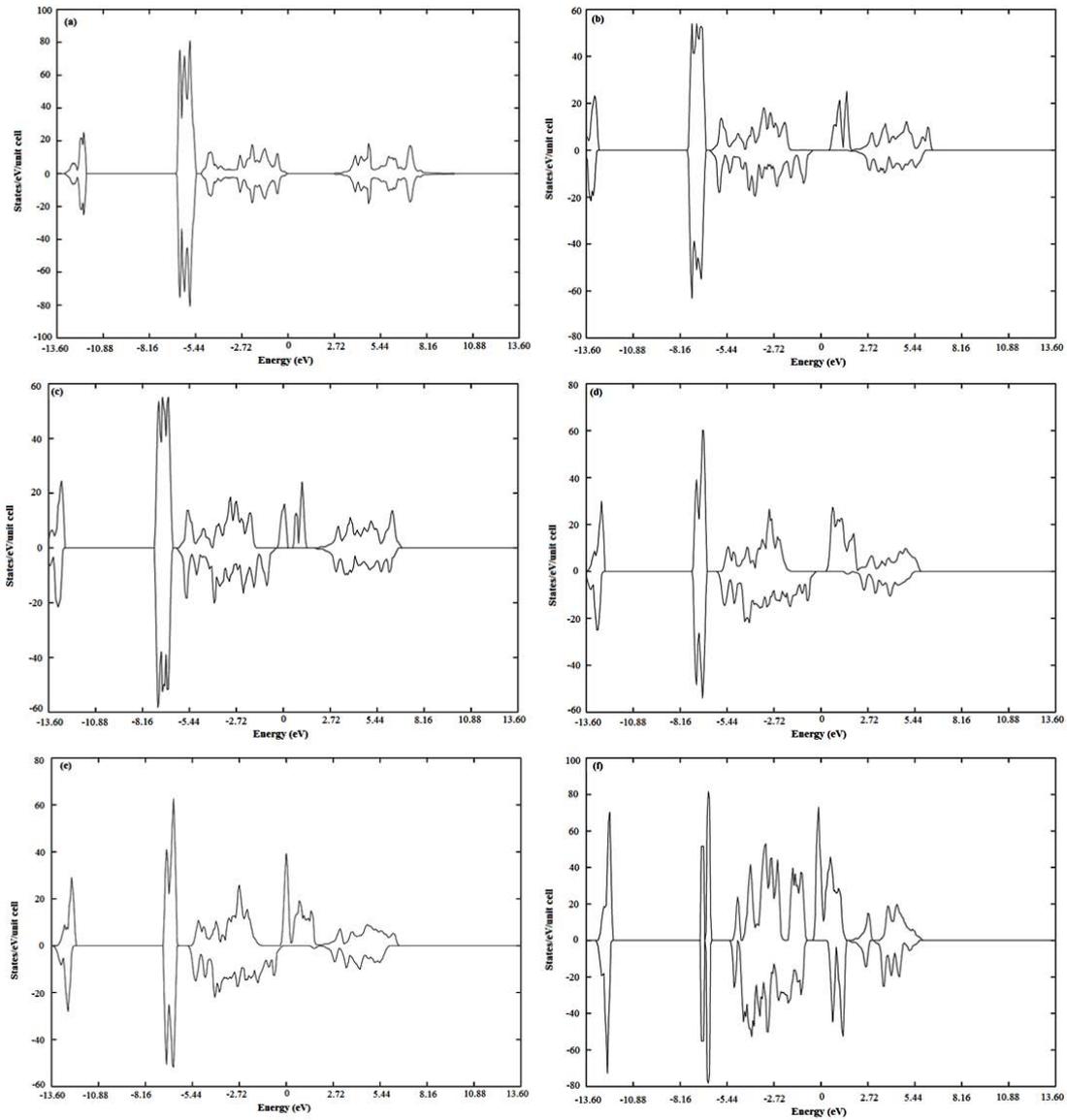
Fig. 5 Spin polarized density of states (DOS) for ZnS and ZnFeS (a) un-doped, (b) 3.125% Fe, (c) 6.25% Fe, (d) 9.375% Fe, (e) 12.50% Fe and (f) 15.625% Fe

REFERENCES

Akai, H. (1998), "Ferromagnetism and Its Stability in the Diluted Magnetic Semiconductor (In, Mn)As," *Phys. Rev. Lett.*, **81**, 3002-3005.

Akai, H., Kamatani, T. and Watanabe, S. (2000), "Electronic structure of diluted magnetic semiconductors and their superlattices," *J. Phys. Soci. Japan,* **69**, 119-124.

Bayer, A., Boyle, D. S. and O'Brien, P. (2002), "In situ kinetic studies of the chemical bath deposition of zinc sulfide from acidic solutions," *J. Mater. Chem.,* **12**(10), 2940-2944.

Cao, J., Han, D. L., Wang, B. J., Fan, L., Fu, H., Wei, M. B. and Yang, J. H. (2013), "Low temperature synthesis, photoluminescence, magnetic properties of the transition metal doped wurtzite ZnS nanowires," *J. Solid State Chem.,* **200**, 317-322.

Chauhan, R., Kumar, A. and Chaudhary, R. P. (2013), "Structural, optical and photocatalytic studies of Fe doped ZnS nanoparticles," *J. Sol-Gel Sci. Techn.,* **67**(2), 376-383.

Chen, H. X., Shi, D. N., Qi, J. S. and Wang, B. L. (2011), "First-principles study on the magnetic properties of transition-metal atoms doped (ZnS)(12) cluster," *J. Magn. Magn. Mater,* **323**(6), 781-788.

Datta, A., Panda, S. K. and Chaudhuri, S. (2008), "Phase transformation and optical properties of Cu-doped ZnS nanorods," *J. Solid State Chem.,* **181**(9), 2332-2337.

Dietl, T., Ohno, H., Matsukura, F., Cibert, J. and Ferrand, D. (2000), "Zener Model Description of Ferromagnetism in Zinc-Blende Magnetic Semiconductors," *Science,* **287**(5455), 1019-1022.

Hohenberg, P. and Kohn, W. (1964), "Inhomogeneous Electron Gas," *Phys. Rev.,* **136**(3B), B864-B871.

Holub, M., Chakrabarti, S., Fathpour, S., Bhattacharya, P., Lei, Y. and Ghosh, S. (2004), "Mn-doped InAs self-organized diluted magnetic quantum-dot layers with Curie temperatures above 300 K," *Appl. Phys. Lett.,* **85**(6), 973-975.

Kataoka, T., Kobayashi, M., Sakamoto, Y., Song, G. S., Fujimori, A., Chang, F.-H. and Dasgupta, I. (2010), "Electronic structure and magnetism of the diluted magnetic semiconductor Fe-doped ZnO nanoparticles," *J. Appl. Phys.,* **107**(3).

Kohn, W. and Sham, L. J. (1965), "Self-Consistent Equations Including Exchange and Correlation Effects," *Phys. Rev.,* **140**(4A), A1133-A1138.

Li, Y. A., Cao, C. B. and Chen, Z. (2011), "Magnetic and optical properties of Fe doped ZnS nanoparticles synthesized by microemulsion method," *Chem. Phys. Lett.,* **517**(1-3), 55-58.

Martínez, B., Sandiumenge, F., Balcells, L., Arbiol, J., Sibieude, F. and Monty, C. (2005), "Structure and magnetic properties of Co-doped ZnO nanoparticles" *Phys. Rev. B,* **72**(16), 165202.

McNorton, R. D., Schuler, T. A., MacLaren, J. M. and Stern, R. A. (2008), "Systematic trends of first-principles electronic structure computations of $Zn_{(1-x)}A_{(x)}B$ diluted magnetic semiconductors," *Phys. Rev. B,* **78**(7).

Nie, E. Y., Liu, D. L., Zhang, Y. S., Bai, X., Yi, L., Jin, Y. and Sun, X. S. (2011), "Photoluminescence and magnetic properties of Fe-doped ZnS nano-particles synthesized by chemical co-precipitation," *Appl. Surf. Sci.,* **257**(21), 8762-8766.

Ohno, H., Shen, A., Matsukura, F., Oiwa, A., Endo, A., Katsumoto, S. and Iye, Y. (1996), "(Ga,Mn)As: A new diluted magnetic semiconductor based on GaAs," *Appl. Phys. Lett.,* **69**(3), 363-365.

Perdew, J. P., Burke, K. and Ernzerhof, M. (1996), "Generalized Gradient Approximation Made Simple," *Phys. Rev. Lett.,* **77**(18), 3865-3868.

Sambasivam, S., Joseph, D. P., Reddy, D. R., Reddy, B. K. and Jayasankar, C. K. (2008), "Synthesis and characterization of thiophenol passivated Fe-doped ZnS nanoparticles," *Mat. Sci. Eng. B- Solid,* **150**(2), 125-129.

Stern, R. A., Schuler, T. M., MacLaren, J. M., Ederer, D. L., Perez-Dieste, V. and Himpsel, F. J. (2004), "Calculated half-metallic behavior in dilute magnetically doped ZnS," *J. Appl. Phys.,* **95**(11), 7468-7470.

Wei, M. B., Yang, J. H., Yan, Y. S., Cao, J., Zuo, Q. H., Fu, H. and Fan, L. (2013), "The investigation of the maximum doping concentration of iron in zinc sulfide nanowires, and its optical and ferromagnetic properties," *Superlattice Microst,* **54**, 181-187.

Xie, J. M. (2010),"First-principles study on the magnetism in ZnS-based diluted magnetic semiconductors,"*J. Magn Magn Mater,* **322** (19), L37-L41.

Zhu, F., Dong, S. and Yang, G. D. (2010), "Ferromagnetic properties in Fe-doped ZnS thin films," *Optoelectron.Advan. Mater.,* **4**(12), 2072-2075.